J Mater Sci (2012) 47:8234–8244
DOI 10.1007/s10853-012-6720-8

Vessel diameter and liquid height dependent sonication-assisted production of few-layer graphene

Min Yi · Zhigang Shen · Xiaojing Zhang · Shulin Ma

Received: 27 March 2012 / Accepted: 4 July 2012 / Published online: 18 July 2012

Abstract Sonication-assisted liquid-phase exfoliation of graphite makes facile, scalable, and low-cost graphene production possible, but there is little information about how sonication-related factors such as vessel diameter (D) and liquid height (H) affect this process and how to scale-up this technique. In this article, the dependence of the sonication-assisted few-layer graphene (FLG) production on D and H was investigated based on experiments and numerical simulation which was performed by finite element method to determine cavitation-related parameters. It was found that by essentially changing the cavitation phenomenon, D and H could critically affect the FLG concentration, FLG yield, injected power, and production efficiency. Combined experimental and simulational analyses reveal that though D and H can change both cavitation volume and cavitation volume fraction, it is the cavitation volume fraction that directly relates to the FLG concentration and production efficiency with a monotonically increasing trend, while the FLG yield and injected power are almost proportional to the cavitation volume, which in turn follows a linear increasing trend with the sample volume. The practical importance for industrial FLG production may lie in the following: (1) D and H should be carefully designed to obtain high cavitation volume fraction to gain high production efficiency and FLG concentration or output-input ratio and (2) large D, H, or sample volume is necessary for achieving large cavitation volume to enhance the FLG yield. Moreover, enhancement in pressure amplitude or cavitation intensity could also favor FLG production. These results have verified the importance of D and H which are often ignored when studying graphene production, and will provide important information on designing large-sized vessels for mass-producing graphene by sonication.

M. Yi · Z. Shen (✉) · X. Zhang · S. Ma
Beijing Key Laboratory for Powder Technology Research & Development, Ministry-of-Education Key Laboratory of Fluid Mechanics, Beijing University of Aeronautics and Astronautics, 37 Xueyuan Road, Beijing 100191, China
e-mail: shenzhg@buaa.edu.cn

Introduction

Graphene has been fascinating worldwide researchers due to its extraordinary properties and bright prospects in numerous fields [1, 2]. Since graphene was successfully prepared in 2004 [3], graphene production has always been a critical issue in bringing graphene to the real-world applications. Currently, there are a large number of methods proposed to prepare graphene [4–16], among which the direct liquid-phase exfoliation of natural graphite flakes shows superiority and makes facile, scalable, and low-cost graphene production possible [8, 10, 12–14]. This exfoliation process in liquid phase is generally accomplished via sonication which plays a crucial role in this technique [7, 9, 11, 17, 18]. As a unique and innocuous irradiation, sonication appears to be vastly superior to other mechanical energies in many applications [17–20] and contributes to exfoliating laminated graphite and the formation of stable graphene dispersion [7, 9, 11, 17, 18].

As we know, it is cavitation brought about by sonication in liquids that results in shock waves and micro-jets to exfoliate flaked graphite into graphene [17, 18, 21, 22]. However, the distribution and intensity of the sonication-induced cavitation are highly dependent on the vessel size and shape which often induce localized cavitation pictures [23–27]. Thus, the vessel size and shape are bound to affect the sonication-assisted production processes of graphene such as exfoliation degree of graphite, graphene concentration, graphene

yield, production efficiency, etc. Though a great many researchers have experimentally demonstrated sonication-based graphene preparation as previously published [8, 10], these publications do not pay enough attention to the vessels in which sonication happens to produce graphene. In addition, the lack of details about geometry and position of vessels in these publications hinders the comparison of experimental results such as graphene concentration and production efficiency between each other. It sometimes even leads to a contradiction or great disparity in these results. In fact, some researchers have noted that the final graphene concentration is largely affected by vessel geometry and dispersion volume [28, 29]. Nevertheless, presently, little thorough information on the effect of these parameters on the sonication-assisted graphene production is available. So, it is necessary to distinctly address this issue.

In addition, because sonication-assisted production of graphene shows potential and practicability in mass-producing liquid-phase processable graphene for industrial applications [8], the knowledge on the scale-up of the sonicated vessels is indispensable. However, it is our understanding that the scale-up effects in graphene production have not been sufficiently investigated. And, very little is known about the effect of sonication-relative parameters on the graphene production process. Moreover, as sonication-sensitive parameters, vessel diameter (D) and liquid height (H) should be mandatorily changed and redesigned when taking the set-up from laboratory to industry. Hence, in order to scale-up the sonicated vessels for mass-producing graphene, it is important and necessary to elucidate the effect of D and H on this sonication-based technique, thus guiding the construction of sonicated vessels on an industrial scale.

The present work aims at investigating the effect of D and H on the sonication-assisted few-layer graphene (FLG) production. FLG dispersion was prepared by sonicating graphite in cyclohexanone with a varied H and D. Sonication-induced pressure fields in these vessels were predicted by the finite element method (FEM) to determine the cavitation distribution and cavitation-related parameters. The dependence of FLG concentration, FLG yield, injected power, production efficiency, and cavitation-related parameters (cavitation volume and cavitation volume fraction) on D and H was also analyzed. These results not only elucidate the importance of D and H in the sonication-assisted production of graphene, but also provide essential information for designing large-sized vessels for industrial applications.

Experimental

Equipment and preparation

The sketch of the experimental set-up designed for preparing FLG by sonicating graphite in cyclohexanone is presented in Fig. 1a. Cylindrical stainless steel vessels with a flat 1.5-mm-thick base, a 1-mm-thick wall, and six different diameters (Φ20, 30, 40, 60, 80, 100 mm) were used for holding dispersion as shown in Fig. 1c. The sonic bath (KX-1620HG, Beijing Kexi, China) worked under air atmosphere with a Φ50 mm oscillator which was operated at 80 W and 28 kHz. In studying the effect of D, H was standardized at 30 mm. While studying the effect of H, the Φ30 mm vessel was chosen and H was set as 22, 30, 43, 54, 65, 73 mm.

By measuring the temperature rise of a known mass of water in these vessels sonicated for various times, the power injected into the liquid inside the vessels was calculated by Power $= (dT/dt)C_p m$ where dT/dt is the temperature rise per second, C_p is the specific heat capacity of water (4.2 J/g/K),

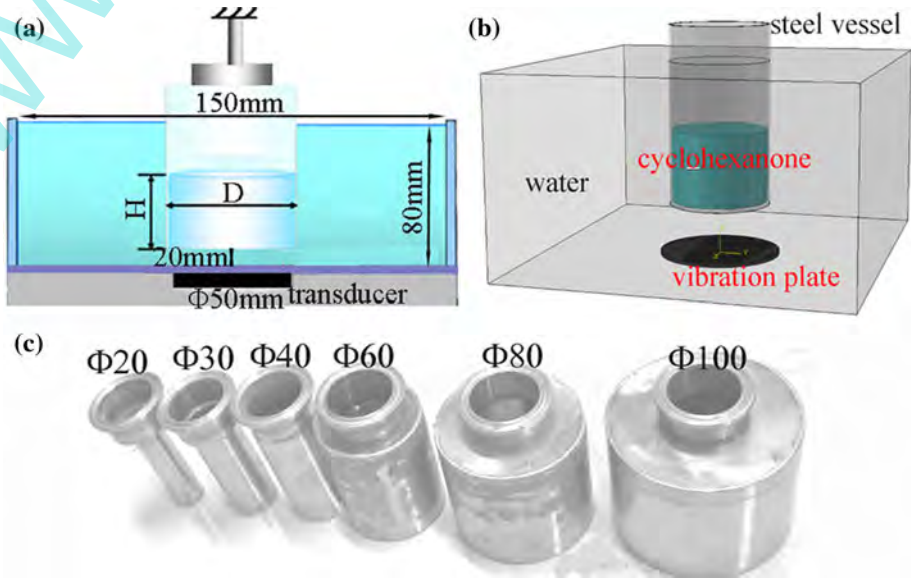

Fig. 1 **a** Schematic of the experimental set-up where $D = 20, 30, 40, 60, 80, 100$ mm when H maintains 30 mm and $H = 22, 30, 43, 54, 65, 73$ mm when D maintains 30 mm. **b** Model used for FEM calculation. **c** Photograph of the vessels used for all the experiments

and m is the mass of water in the vessel [30]. The temperature was monitored at room temperature using a thermocouple.

The initial concentration of graphite in cyclohexanone is 0.5 mg/mL. After 60 min of sonication, the obtained dark dispersion was left to stand for 12 h for sufficient sedimentation of large particles. Then, the upper less dark dispersion was centrifuged at 3,000 rpm (1,280×g) for 30 min with a centrifuge (L-600, Changsha XiangYi, China) to remove any largish flakes, eventually resulting in homogeneous colloidal suspension of graphene sheets in cyclohexanone. For each experimental case, seven samples were repeated. Optical absorbance measurements were performed at 660 nm using a Vis spectrophotometer (721E, Shanghai Spectrum, China) with a 1 cm cuvette. And, the concentration C_G after centrifugation was determined from Lambert–Beer law, $A/l = \alpha C_G$, where α was taken as 2,460 mg/mL/m [31]. Height profile and morphology of graphene sheets were investigated with AFM CSPM5500 (Being Nano-Instruments, China) equipped with a 13.56 μm scanner in tapping mode. Transmission electron microscopy (TEM) and high resolution TEM (HRTEM) imaging were performed using a JEOL JEM-2010FEF operated at 200 kV.

Numerical simulations

Theoretical prediction of cavitation activity in terms of pressure distribution was made by solving the linear steady-state wave equation by FEM, where the coupling between the acoustic field of the liquid and the vibration of the vessel's wall was considered. If linear wave propagation in a homogeneous media is assumed and the shear stress is neglected (which is correct for liquids and gases), the wave equation has this form:

$$\frac{1}{\rho}\nabla^2 P - \frac{1}{\rho c^2}\frac{\partial^2 P}{\partial t^2} = 0 \quad (1)$$

where P is the acoustic pressure, ρ is the density, and c is the speed of the sound. The transducer works at a constant frequency ($f = 28$ kHz) so the pressure P is considered time harmonic, i.e.,

$$P(r, t) = p(r)e^{i\omega t} \quad (2)$$

where spatial variable $r = r(x, y, z)$ and $\omega = 2\pi f$. Hence, the space-dependent steady-state wave equation is

$$\frac{1}{\rho}\nabla^2 p + \frac{\omega^2}{\rho c^2}p = 0 \quad (3)$$

where $p = p(x, y, z)$ is the pressure amplitude at position (x, y, z).

In the present study, ABAQUS software has been utilized to perform the simulation. The model used for FEM calculation in ABAQUS is shown in Fig. 1b. In Table 1, the physical quantities of the materials used in these calculations are listed. The boundary conditions were assigned as follows. The upper edge of the vessel was fixed. $p = 0$ was applied to the upper boundary edge where water and cyclohexanone were in contact with atmosphere. The container holding water was assumed to have rigid walls so $\partial p/\partial n = 0$ was applied to the water surfaces which touch the container's wall. As for the steel vibration plate for irradiating ultrasound, uniform displacement amplitude $u_0 = 0.5$ μm was applied. The acoustic-structural coupling between liquid and steel was defined by means of a surface-based coupling procedure embedded in ABAQUS. Direct steady-state dynamics method in ABAQUS/Standard was adopted to obtain the distribution of pressure amplitude in cyclohexanone and water at $f = 28$ kHz.

Based on the distribution of pressure amplitude, cavitation distribution could be roughly determined. Under the temperature of the experimental condition, the vapor pressure of cyclohexanone is several hundred Pa (~670 Pa at 25 °C). Moreover, in the actual experiment, the presence of graphite dispersed into cyclohexanone, and more especially the occurrence of trapped vapor–gas nuclei in the crevices and recesses of these graphite particles, can appreciably lower the cavitation threshold of cyclohexanone [32]. Theoretically, bubbles form and cavitation happens when the pressure difference (acoustic pressure generated by sonication minus atmospheric pressure) is less than vapor pressure [32]. So, with atmospheric pressure (~1.01325 bar) considered, it can be approximately thought that cavitation happens in these regions where the absolute value of pressure amplitude exceeds 1.1 bar. In addition, a FORTRAN program was constructed to process the data output from ABAQUS in order to determine the cavitation volume and cavitation volume fraction in cyclohexanone in each simulational case.

Results

FLG in cyclohexanone

With its surface tension and Hansen solubility parameters matching those of graphene, cyclohexanone is deemed as

Table 1 The physical properties of materials used in the present calculations[a]

Material	E (GPa)	B (GPa)	υ	ρ (g/cm^3)	c (m/s)
Water	–	2.23	–	0.997	1,496
Cyclohexanone	–	1.88	–	0.948	1,407
Steel	195	–	0.3	7.7	–

[a] E, B, υ denote Young's modulus, bulk modulus, Poisson ratio, respectively. $c = (E/\rho)^{1/2}$ or $(B/\rho)^{1/2}$

an excellent solvent for exfoliating graphite and dispersing graphene [31]. To provide evidence that FLG was really prepared in cyclohexanone by sonication, Fig. 2 gives representative AFM and TEM images of the prepared FLG. The step height of 0.8 nm in Fig. 2a indicates a graphene sheet of no more than 3 layers. The root-mean-square surface roughness of the sheet is about 0.1 nm, which approaches the noise limit of the instrument. Figure 2b shows more FLG sheets with a thickness of $\sim$1 nm. In addition, Fig. 2d gives a FLG sheet the layer number of which can be estimated as four by the HRTEM image of edge fringe in Fig. 2e. Graphene sheets captured by TEM are generally with a lateral size of micrometer order as shown in Fig. 2d. This may be attributed to the fact that submicrometer graphene sheets may leak out through the TEM grid. We have also tried to distinguish the distribution of thickness and lateral size of FLG sheets prepared in a different D and H based on TEM and AFM, but no firm evidence and regular results were obtained. Because, graphene sheets captured and analyzed by TEM and AFM only occupy an extremely small portion of the prepared dispersion so that the sample volume used for characterization is too small to reach a solid conclusion. Hence, the differences between individual FLG sheets will not be addressed in this study.

Pressure field and cavitation-related parameters

The pressure field in cyclohexanone for all the experimental cases was predicated by FEM simulation. The complete profiles for the distribution of the pressure field in cyclohexanone with D and H are depicted in Figs. 3 and 4. It can be easily seen from these figures that the maximum pressure amplitude is several bars and the pressure field is extremely nonuniform even in the simulational case with the minimum volume. It should be noted that the presented simulational results in Figs. 3 and 4 only give the absolute value of pressure amplitude of each position, the transient pressure of which is actually time harmonic as shown in expression (2). Cavitation volume and cavitation volume fraction are taken as two cavitation phenomenon-related parameters to study the effect of D and H. Based on the criterion in the experimental section that cavitation happens when the absolute value of pressure amplitude exceeds 1.1 bar, a FORTRAN program was utilized to process the FEM results to calculate the cavitation volume and cavitation volume fraction as shown in Figs. 5 and 6. Cavitation volume is the volume of liquid where cavitation happens; while dividing cavitation volume by the total liquid volume gets the cavitation volume fraction. In Fig. 5, the cavitation volume increases with increasing D

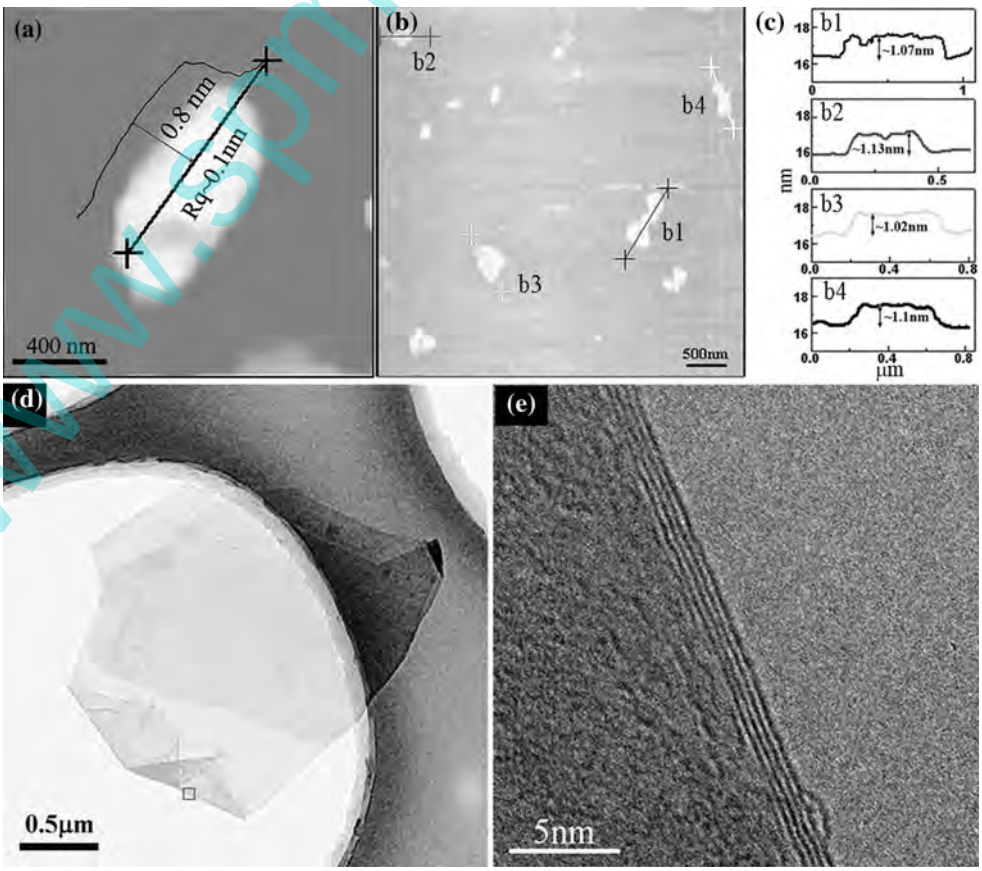

Fig. 2 **a** An AFM image of an FLG sheet. **b** An AFM image with several FLG sheets. **c** Height profiles obtained from positions indicated in (**b**). **d** A bright field TEM image of a folded FLG sheet. **e** A HRTEM image of a folded edge indicated by a *square* in (**a**)

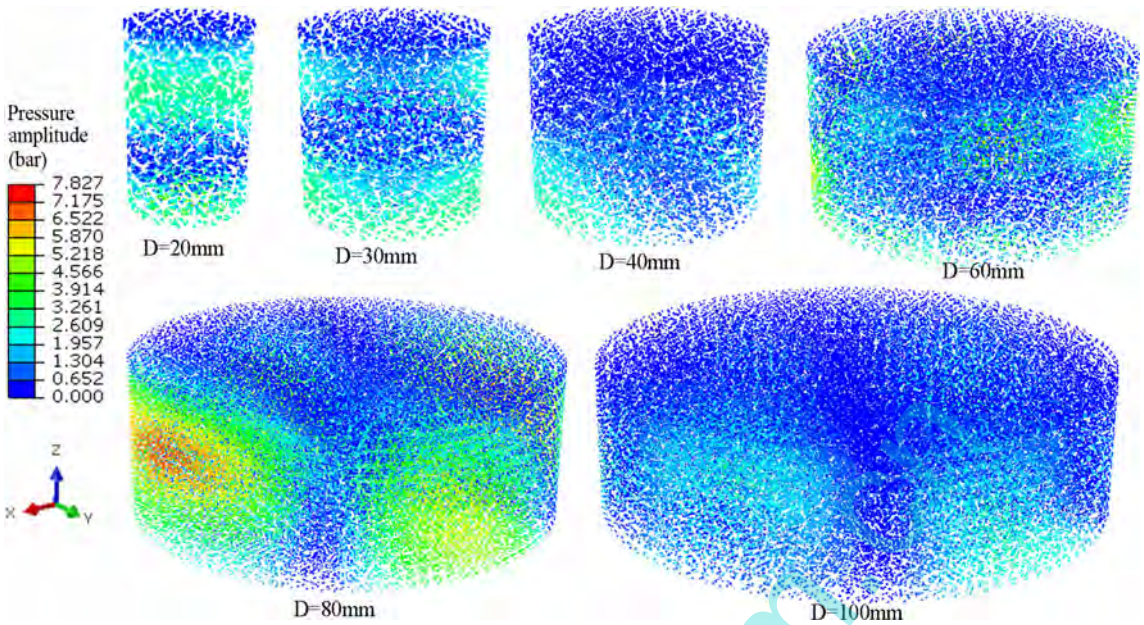

Fig. 3 Simulational sonication-induced pressure field distribution of experiment cases with $H = 30$ mm and $D = 20, 30, 40, 60, 80, 100$ mm. All the elements are shrunk for better visualization and the pressure amplitude is shown as the absolute value

and then slightly decreases when D is over 80 mm, but with two "outliers," the increasing tendency with H is less remarkable.

FLG concentration, yield and injected power

Figure 6 shows the FLG concentration which wildly fluctuates with the variation of D and H. These results also obviously deviate from the reported FLG concentration of 7.3 μg/mL [31] because many factors such as vessel geometry could affect the FLG production, i.e., an issue investigated here. It can be seen that among all the experimental cases in this study, the highest FLG concentration reaches ~19.2 μg/mL, while the lowest is only ~6.1 μg/mL. The great difference in FLG concentrations implies the necessity of investigating the effect of D and H on the FLG production.

Multiplying the measured FLG concentration C_G (μg/mL) by the total sample volume (cm^3) which is calculated by $\pi(D/2)^2H$, the FLG yield of each experimental case can be obtained as shown in Fig. 7a. It is found that the FLG yield exhibits a tendency to increase as D or H increases, though one or two "outliers" exist and the increase rate varies acutely.

Based on the calorimetry measurement referred in the experimental section, Fig. 7b gives the power injected into the vessel as a function of D or H. It can be seen that the injected power increases with increasing D and H, although the same output power from the sonicator was applied to all vessels.

Discussion

FLG concentration

The FLG concentration is a significant reference for both evaluating a solvent and estimating FLG yield. In this study, the effect of D and H on the FLG concentration was investigated as shown in Fig. 6. Clearly, the deviation of FLG concentration is great among the different experimental cases, though the same sonicator, sonication time, and centrifugation condition were used. This reveals the indispensability to consider D and H when comparing results from experiments, the other experimental conditions of which are the same. However, so far, this issue has been paid little attention, and the absence of information on D and H may make the comparison between the reported results from the same solvent-based experiments invalid.

In addition, as shown in Fig. 6, the variation of cavitation volume fraction with D and H presents the same trend as exhibited in the variation of FLG concentration. This indicates a strong correlation between experimental and simulational data. This also illustrates that the FLG concentration is highly dependent on or nearly determined by cavitation volume fraction. In order to discern this correlation, the dots of cavitation volume fraction versus FLG concentration are plotted in Fig. 8a. From the scope of sole square-dot sequence or sole circle-dot sequence in Fig. 8a, it can be observed that the FLG concentration monotonically increases with cavitation volume fraction. Taking D/H, i.e., aspect ratio, as the geometry parameter, cavitation volume fraction and FLG concentration also show the same trend with

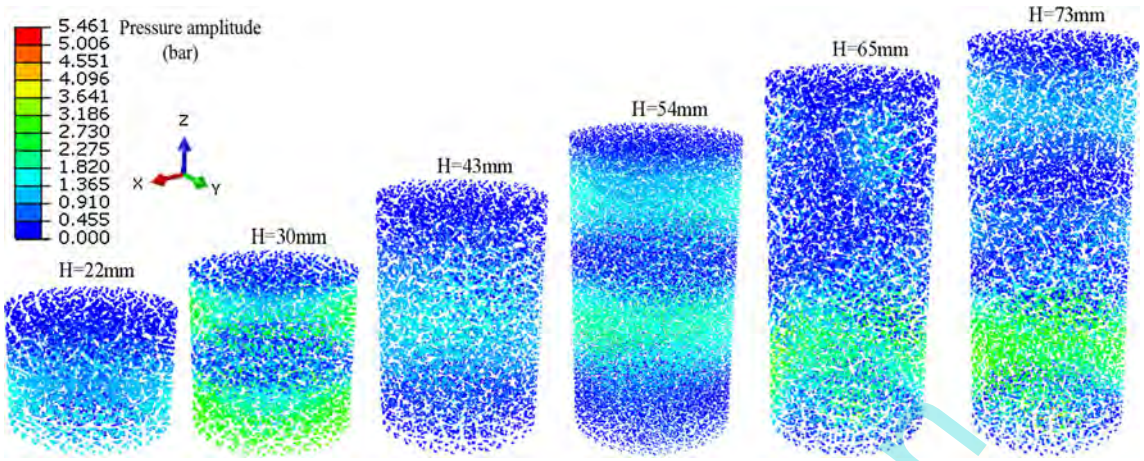

Fig. 4 Simulational sonication-induced pressure field distribution of experiment cases with $D = 30$ mm and $H = 22, 30, 43, 54, 65, 73$ mm. All the elements are shrunk for better visualization and the pressure amplitude is shown as the absolute value

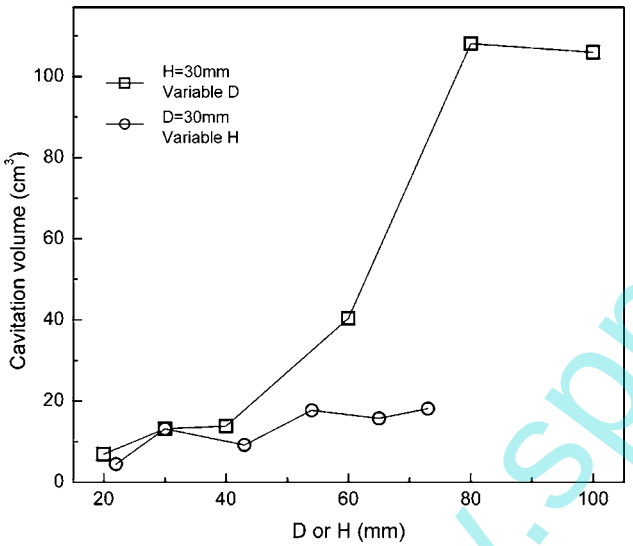

Fig. 5 Cavitation volume calculated from FEM results based on a FORTRAN program as a function of D or H

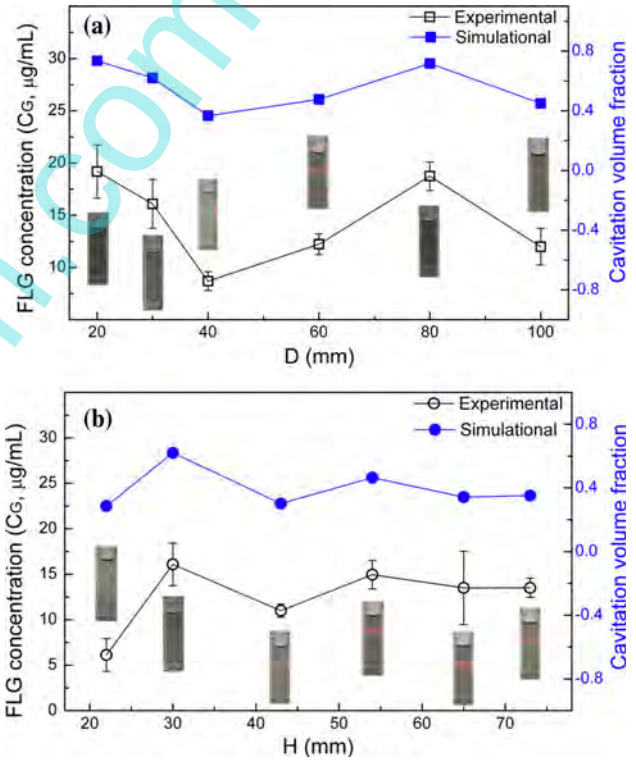

Fig. 6 FLG concentration C_G and cavitation volume fraction calculated from FEM results based on a FORTRAN program as a function of D (**a**) and H (**b**). C_G is shown as hollow dots and cavitation volume fraction as *solid dots*. The Tyndall scattering effect is seen in the *inset* photographs for the FLG dispersion from the corresponding experiment case

variable D/H as presented in Fig. 8b. It is well known that acoustic cavitation of high frequency ultrasound results in the formation, growth, and collapse of microbubbles in solution, and the bubble collapse can induce shock waves and micro-jets on the surface of the bulk graphite to cause exfoliation [17, 18, 21, 22]. And, different D and H, i.e., deferent geometry, will result in different cavitation distribution, namely different cavitation volume and cavitation volume fraction in this study. However, cavitation volume shows no monotonic relation with FLG concentration as depicted in Fig. 8c. Therefore, it can be concluded that though the D and H, i.e., D/H, can change both cavitation volume and cavitation volume fraction, it is the cavitation volume fraction that directly corresponds to the FLG concentration in the final dispersion. Thus, in order to obtain highly concentrated FLG dispersion or increase the output-input ratio in industrial FLG production, D and H or D/H should be carefully designed to achieve the maximum cavitation volume fraction. Nevertheless, the optimum D/H for the maximum cavitation volume fraction cannot be predicted

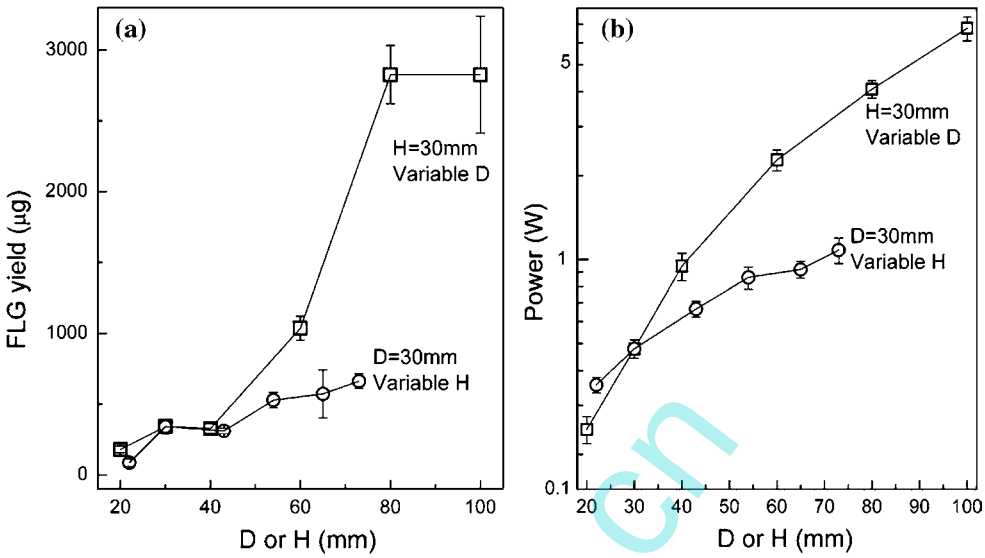

Fig. 7 *Plots* of FLG yield (**a**) and power (**b**) as a function of D or H

here because the cavitation phenomenon is an extremely nonlinear process and is very sensitive to D/H (i.e., a small change in D/H may induce a great change in the cavitation phenomenon) as shown in Fig. 8b with irregular behavior. The design about cavitation volume fraction may depend on trial and error with simulational investigation as an auxiliary.

FLG yield

In contrast to the violently fluctuated FLG concentration, the FLG yield varying with D or H (Fig. 7a) approaches a monotonic trend. But, in Fig. 9a, the FLG yield does not change with cavitation volume fraction monotonically, indicating that the cavitation volume fraction does not determine the yield. So, from this result, it can be interpreted that the cavitation volume or the total sample volume contributes a lot to the final calculated FLG yield despite the violently fluctuated concentration. This can be understood by expounding the relationships among FLG yield, cavitation volume, and total sample volume as shown in Fig. 9b and c. In Fig. 5, as D or H increases for fixed H or D, respectively, the cavitation volume also increases. Compared to the cavitation volume fraction trends in Fig. 6, the increasing sample volume results in a linear increase in the cavitation volume (Fig. 9c). And, the cavitation volume is overlaid with some fluctuations related to D/H (Fig. 9d), i.e., geometry. In short, there is a linear increase trend in FLG yield with an increase in cavitation volume (Fig. 9b), which is in turn approximately proportional to the total sample volume (Fig. 9c). So, it merely says that more sample volume means more FLG in dispersion following a linear trend, and that although aspect ratio D/H changes the cavitation phenomenon and FLG yield, cavitation volume rather than cavitation volume fraction is proportional to the FLG yield. Unlike cavitation volume fraction, cavitation volume approximately presents

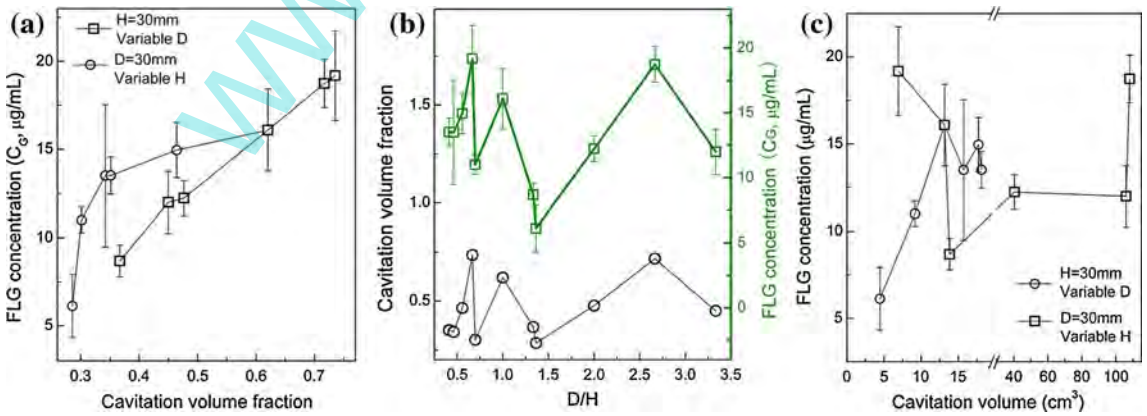

Fig. 8 **a** FLG concentration as a function of cavitation volume fraction. **b** Cavitation volume fraction and FLG concentration as a function of D/H. **c** FLG concentration as a function of cavitation volume

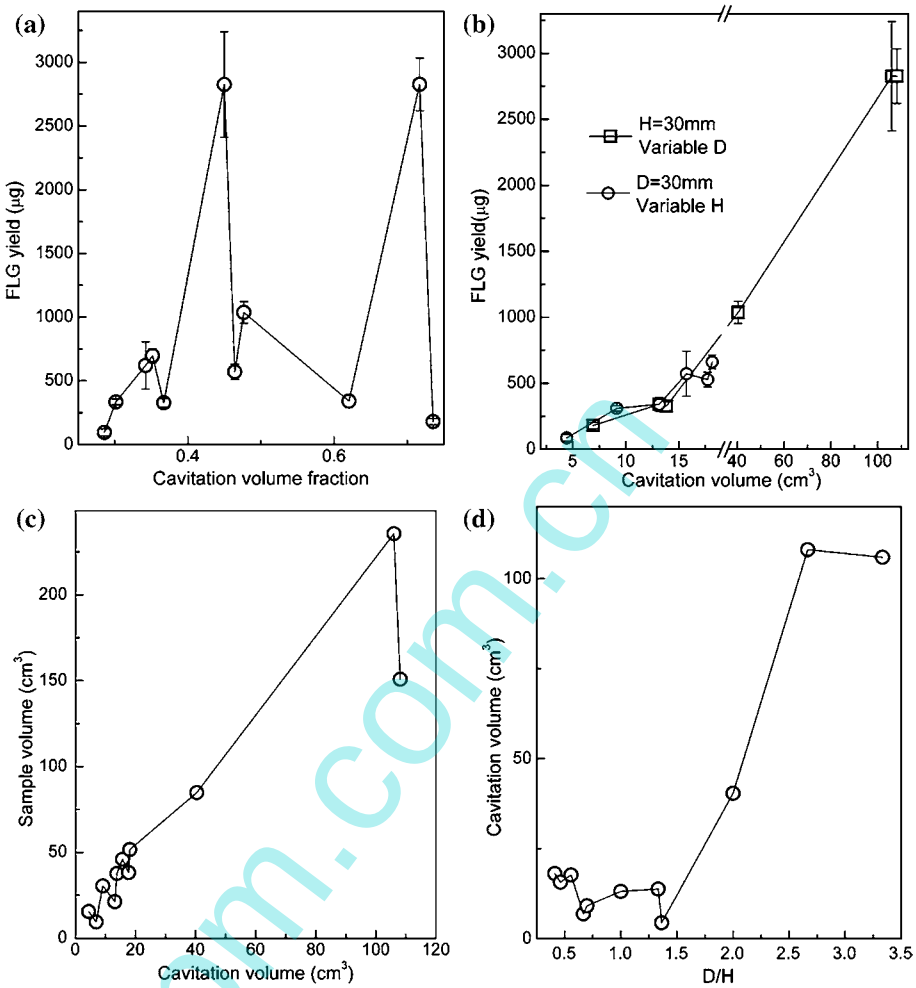

Fig. 9 *Plots* of **a** FLG yield versus cavitation volume fraction, **b** FLG yield versus cavitation volume, **c** sample volume versus cavitation volume, and **d** cavitation volume versus D/H

a linear trend with D, H, sample volume, and D/H, indicating a regular and predictable behavior. Hence, when considering vessel geometry or D/H for large-scale production of FLG, a large quantity of cavitation volume, which can be realized by large D, H, D/H, or sample volume, is necessary.

Production efficiency

Before discussing the production efficiency, we firstly discuss the effect of D and H or aspect ratio D/H on the injected power as shown in Fig. 10a. The injected power nearly presents an increasing trend with variable D/H. To explain this, it should be remembered that the injected power is related to the cavitation phenomenon during which cavitation bubbles collapse to release energy to heat the liquid. So, the injected power must highly depend on the cavitation volume and sample volume just as evidenced in Fig. 10b with a linear increasing trend. This means that as sample volume increases, more power is absorbed.

Production efficiency is an essential parameter for evaluating the performance of a set-up for producing FLG. In sonochemistry, it has been known that the sonochemical efficiency is sensitively affected by the experimental conditions where the injected energy and sample volume would be the most important factors [27]. Similarly, these factors should also affect the production efficiency in the sonication-based production of FLG. According to the calculation method which is widely used to define sonochemical efficiency or cavitation efficiency in sonochemistry [33, 34], the production efficiency in this study can be calculated by dividing the FLG yield by the injected energy (power × time) as presented in Fig. 10c. It can be found that the trend of the production efficiency varying with D and H is the same as that of the FLG concentration in Fig. 6. This indicates that the production efficiency is also a quantity strongly dependent on the cavitation volume fraction as evidenced in Fig. 10d. Therefore, like the case of FLG concentration, the designed geometry should have the proper D, H, or D/H to achieve a high cavitation

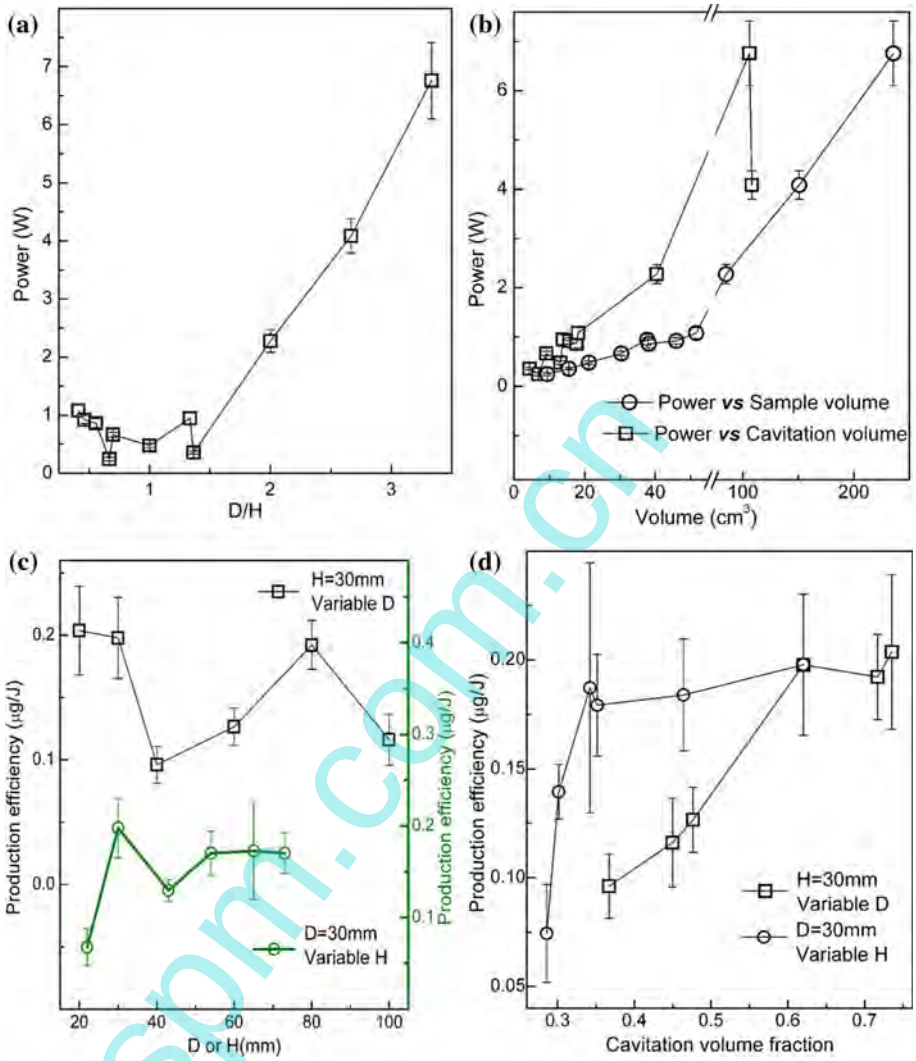

Fig. 10 *Plots* of **a** power versus D/H, **b** power versus sample volume and cavitation volume, **c** production efficiency versus D or H, and **d** production efficiency versus cavitation volume fraction

volume fraction in terms of high production efficiency in large-scale FLG production.

Additional remarks on cavitation intensity

Though the fact that the above-discussed experimentally determined parameters (FLG concentration, FLG yield, injected power, production efficiency) are strongly dependent on the simulation-determined cavitation volume or cavitation volume fraction has been confirmed, one troublesome topic should also be pointed out. If all the square and circle dots are inspected as a whole, as shown in Fig. 11, the above-mentioned monotonic increasing tendency is discounted. This suggests that there are other factors within cavitation phenomenon affecting the production efficiency and FLG concentration besides cavitation volume and cavitation volume fraction. It should be remembered that in this study, only cavitation volume and cavitation volume fraction are taken as cavitation phenomenon-related parameters which are affected by D and H. Actually, cavitation intensity is also an important factor because a different pressure amplitude could induce cavitation with a different intensity, thus leading to stress waves of different stress amplitude in the bulk graphite [35–38]. For example, in Fig. 11, the case with $D = 40$ mm and $H = 30$ mm gives a cavitation volume fraction of $\sim$36.7 % and an FLG concentration of $\sim$8.7 μg/mL, but the case with $D = 30$ mm and $H = 73$ mm results in slightly less cavitation volume fraction ($\sim$35.2 %), but a much higher FLG concentration ($\sim$13.5 μg/mL). This abnormal result seems to contradict the monotonic trend of FLG concentration varying with cavitation volume fraction. However, this result is simply obtained when the magnitude of pressure amplitude of positions where pressure amplitude is larger than 1.1 bar is ignored. In other words, once the pressure amplitude of some positions is greater than 1.1 bar and no matter how large the pressure amplitude is, the cavitation intensity in these positions is taken as the same. But, as mentioned above, the fact is that a larger pressure amplitude will induce a more intensive cavitation. Therefore, a reference pressure amplitude of

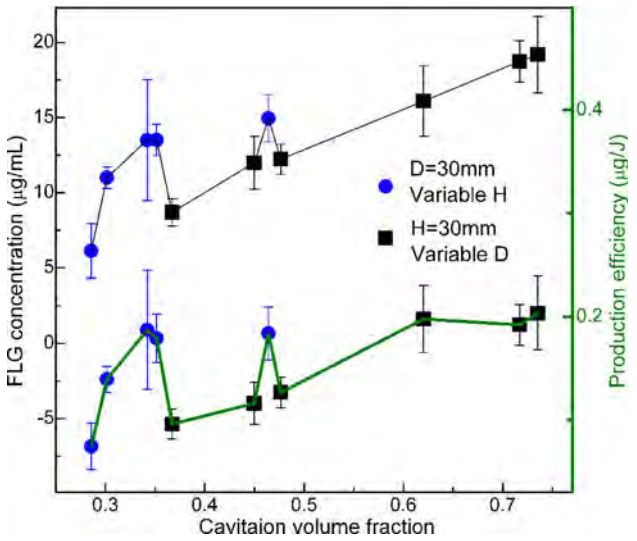

Fig. 11 *Plot* of FLG concentration and production efficiency as a function of cavitation volume fraction combining all the *square* and *circle dots* in one *plot*

1.1 bar is invalid because it reaches the above-mentioned abnormal result. So, a larger reference pressure amplitude is needed to qualitatively expound this issue, for instance, 2 bar. Based on these clarifications, if the magnitude of the pressure amplitude of positions where cavitation happens is considered, it can be obtained that ~52.3 % of the cavitation region in the case with $D = 30$ mm, $H = 73$ mm has a pressure amplitude of more than 2 bar, while only ~19.6 % in the case with $D = 40$ mm, $H = 30$ mm. Hence, if this cavitation intensity correction is considered, the abnormal phenomenon between case $D = 40$ mm, $H = 30$ mm and case $D = 30$ mm, $H = 73$ disappears and the monotonic trend is still valid. This simple qualitative analysis indicates the effect of cavitation intensity responsible for the discounted increasing tendency in Fig. 11 because a larger pressure amplitude will generate a more intense cavitation and stress waves of a higher stress amplitude in the bulk graphite, thus resulting in a higher concentration or production efficiency. However, the relation between pressure amplitude and cavitation intensity is generally extremely complicated and is affected by many factors such as temperature, bubble nuclei radius, bubble distribution, and so on [35–38]. Hence, the quantitative relation between FLG concentration (or production efficiency) and cavitation intensity via pressure amplitude can hardly be established within the FEM model here. Nevertheless, it can be affirmed that cavitation intensity or pressure amplitude could also affect FLG production. A detailed investigation on this issue needs cavitation dynamics simulation and a more sophisticated cavitation model, which are out of the scope here and must be studied in the near future.

Conclusions

In conclusion, the present work has addressed the dependence of sonication-assisted FLG production on D and H based on experiments and numerical simulation. The experimentally determined parameters (FLG concentration, FLG yield, injected power, and production efficiency) and simulation-determined cavitation-related parameters (cavitation volume and cavitation volume fraction) have been investigated to elucidate this dependence. Essentially, by changing the cavitation phenomenon in the vessels, D and H or D/H can critically affect the sonication-assisted FLG production. With the variation of D or H, FLG concentration and production efficiency fluctuate wildly and show irregular behavior which can hardly be predicated, while graphene yield approached a linear increasing trend. Combined experimental and simulational analyses reveal that though D and H or D/H can change both cavitation volume and cavitation volume fraction, it is the cavitation volume fraction that directly corresponds to the FLG concentration and production efficiency with a monotonically increasing trend, while the FLG yield and injected power are almost proportional to the cavitation volume, which in turn follows a linear increasing trend with the sample volume. In addition, enhancement in pressure amplitude or cavitation intensity could also favor FLG production. The practical importance may lie in the following: (1) In order to obtain highly concentrated FLG dispersion, increase the output-input ratio, or enhance production efficiency in industrial FLG production, D and H or D/H should be carefully designed to achieve the maximum cavitation volume fraction; (2) when considering vessel geometry or D/H for large-scale production of FLG, a large quantity of cavitation volume, which can be realized by large D, H, D/H, or sample volume, is necessary. The results reported here not only confirm the significance of D and H in producing graphene by sonication, but also provide a meaningful reference to scale-up the experimental set-up for industrial applications.

Acknowledgements This work was supported by the Special Funds for Co-construction Project of Beijing Municipal Commission of Education, the "985" Project of Ministry of Education of China, and the Fundamental Research Funds for the Central Universities.

References

1. Geim AK, Novoselov KS (2007) Nat Mater 6:183
2. Geim AK (2009) Science 324:1530
3. Novoselov KS, Geim AK, Morozov SV, Jiang D, Zhang Y, Dubonos SV, Grigorieva IV, Firsov AA (2004) Science 306:666
4. Inagaki M, Kim YA, Endo M (2011) J Mater Chem 21:3280
5. Chung DDL (2002) J Mater Sci 37:1475. doi:10.1023/A:1014915307738

6. Choi W, Lahiri I, Seelaboyina R, Kang YS (2010) Crit Rev Solid State 35:52
7. Shao G, Lu Y, Wu F, Yang C, Zeng F, Wu Q (2012) J Mater Sci 47:4400. doi:10.1007/s10853-012-6294-5
8. Coleman JN (2009) Adv Funct Mater 19:1
9. Khvostikova O, Hermann H, Wendrock H, Gemming T, Thomas J, Ehrenberg H (2011) J Mater Sci 46:2422. doi:10.1007/s10853-010-5088-x
10. Cui X, Zhang C, Hao R, Hou Y (2011) Nanoscale 3:2118
11. Jang BZ, Zhamu A (2008) J Mater Sci 43:5092. doi:10.1007/s10853-008-2755-2
12. Liu WW, Wang JN (2011) Chem Commun 47:6888
13. Choi E-Y, Choi WS, Lee YB, Noh YY (2011) Nanotechnology 22:365601
14. Shih C-J, Vijayaraghavan A, Krishnan R et al (2011) Nat Nanotechnol 6:439
15. Li B, Zhong W-H (2011) J Mater Sci 46:5595. doi:10.1007/s10853-011-5572-y
16. Yoon S, In I (2011) J Mater Sci 46:1316. doi:10.1007/s10853-010-4917-2
17. Cravotto G, Cintas P (2010) Chem Eur J 16:5246
18. Skrabalak SE (2009) Phys Chem Chem Phys 11:4930
19. Cao JW, Lofaj F, Okada A (2001) J Mater Sci 36:1301. doi:10.1023/A:1004818901119
20. Torres-Sanchez C, Corney JR (2011) J Mater Sci 46:490. doi:10.1007/s10853-010-4944-z
21. Yi M, Li J, Shen Z, Zhang X, Ma S (2011) Appl Phys Lett 99:123112
22. Shen Z, Li J, Yi M, Zhang X, Ma S (2011) Nanotechnology 22:365306
23. Gogate PR, Tayal RK, Pandit AB (2006) Curr Sci India 91:35
24. Sutkar VS, Gogate PR (2009) Chem Eng J 155:26
25. Nanzai B, Okitsu K, Takenaka N, Bandow H, Tajima N, Maed Y (2009) Ultrason Sonochem 16:163
26. Kojima Y, Koda S, Nomura H (1998) Jpn J Appl Phys 37:2992
27. Asakura Y, Nishida T, Matsuoka T, Koda S (2008) Ultrason Sonochem 15:244
28. Khan U, O'Neill A, Lotya M, De S, Coleman JN (2010) Small 6:864
29. Nuvoli D, Valentini L, Alzari V, Scognamillo S, Bon SB, Piccinini M, Illescas J, Mariani A (2011) J Mater Chem 21:3428
30. Mason TJ, Lorimer JP, Bates DM (1992) Ultrasonics 30:40
31. Hernandez Y, Lotya M, Rickard D, Bergin SD, Coleman JN (2010) Langmuir 26:3208
32. Mason TJ, Lorimer JP (2002) Applied sonochemistry: uses of power ultrasound in chemistry and processing. Wiley–VCH, Weinheim
33. Koda S, Kimura T, Kondo T, Mitome H (2003) Ultrason Sonochem 10:149
34. Berlan J, Mason TJ (1992) Ultrasonics 30:203
35. Noltingk BE, Neppiras EA (1950) Proc Phys Soc B 63:674
36. Chen W, Gu C, Zhao K, Shen F (2006) J Mater Sci 41:2151. doi:10.1007/s10853-006-5209-8
37. Niemczewski B (1980) Ultrasonics 18:107
38. Herbert E, Balibar S, Caupin F (2006) Phys Rev E 74:041603